Characteristics of particle emissions and their atmospheric dilution during co-combustion of coal and wood pellets in a large combined heat and power plant

Fanni Mylläri
Aerosol Physics, Faculty of Natural Sciences, Tampere University of Technology, FI-33101 Tampere, Finland.

Liisa Pirjola
Department of Technology, Metropolia University of Applied Sciences, FI-00180, Helsinki, Finland.

Heikki Lihavainen
Atmospheric Composition Research, Finnish Meteorological Institute, FI-00560, Helsinki, Finland.

Eija Asmi
Atmospheric Composition Research, Finnish Meteorological Institute, FI-00560, Helsinki, Finland.
Servicio Meteorológico Nacional, Av. Dorrego 4019, Buenos Aires, Argentina

Erkka Saukko
Aerosol Physics, Faculty of Natural Sciences, Tampere University of Technology, FI-33101 Tampere, Finland.
Present address: Pegasor, Hatanpään valtatie 34c, 33100 Tampere, Finland.

Tuomas Laurila
Climate System Research, Finnish Meteorological Institute, FI-00560, Helsinki, Finland.

Ville Vakkari

Atmospheric Composition Research, Finnish Meteorological Institute, FI-00560, Helsinki, Finland.

Ewan O'Connor
Atmospheric Composition Research, Finnish Meteorological Institute, FI-00560, Helsinki, Finland.

Jani Rautiainen
Helen Oy, FI-00090 Helen, Helsinki, Finland

Anna Häyrinen
Helen Oy, FI-00090 Helen, Helsinki, Finland

Ville Niemelä
Dekati Ltd., Tykkitie 1, 36240 Kangasala, Finland

Joni Maunula
Valmet Technologies Oy, FI-33101 Tampere, Finland

Risto Hillamo
Atmospheric Composition Research, Finnish Meteorological Institute, FI-00560, Helsinki, Finland.

Jorma Keskinen
Aerosol Physics, Faculty of Natural Sciences, Tampere University of Technology, FI-33101 Tampere, Finland.

Topi Rönkkö
Aerosol Physics, Faculty of Natural Sciences, Tampere University of Technology, FI-33101 Tampere, Finland.

Introduction

During next years and decades, global warming will enforce the increase of the share of renewable energy production, such as solar power, wind power, geothermal heat, as well as biogas and biomass for combustion processes. Regarding the most direct substitution of fossil fuels, the utilization of biomass has been seen to be the promising solution, especially in respect of the current infrastructure of energy systems (Strzalka et al. 2017). Therefore, new biomass alternatives for combustion applications, such as oat hulls (Al-Naiema et al. 2015), pulverized olive residues (Jiménez and Ballester 2004), bark, sludge, solid recovered fuel (Vainio et al. 2013), straw (Hansen et al. 1998), waste (Kuuluvainen et al. 2015) and many more have been studied. Compared to fossil fuel combustion, biomass combustion could lower NO_x, SO_x and fossil-CO_2 emissions (Verma et al. 2017) because the biomass typically contains less sulphur and nitrogen. In addition, biomass could lower the particulate matter (PM) emissions. For instance, in circulating fluidized bed boiler (CFB) the PM emissions lowered with the factor of 12 when 50% of coal (by weight) was substituted with biomass (Al-Naiema et al. 2015). However, the utilization of new types of fuels can cause undesirable effects also, e.g. on the boiler operation or on the emissions of power plants.

Implementation of biomass to combustion processes will not be straightforward with boilers designed for fossil fuels. Hence, upgrading of combustion technologies or pre-treatment of the fuels might be required to enable co-combustion of biomass and fossil fuels, during the transition time before new boilers designed for biomass combustion (Madanayake et al. 2017) will largely be taken into use. The problems in biomass combustion are related to boiler operation, such as increased corrosion risk (Pisa and Lazaroiu 2012), bed agglomeration in fluidized bed combustors (FBC) (Sevonius, Yrjas, and Hupa 2014; Piotrowska et al. 2012), grindability of the fuel, fuel moisture, low density of biomass (Madanayake et al. 2017) and deposit formation (Nutalapati et al. 2007; Heinzel et al. 1998). Some of the problems could be solved by leaching, torrefaction and mechanical pre-treatment (grinding and pelletizing) of the biomass (Madanayake et al. 2017) or by ferric sulphate additives to the fuel (Kuuluvainen et al. 2015). Effect of different pelletizing methods to the grindability and combustion of fuel was studied e.g. by Tolvanen et al. (Tolvanen, Keipi, and Raiko 2016) who showed that raw wood pellets had the slowest reaction rate of the studied pellet qualities and that, to achieve similar

reaction rate as other fuels, the raw wood pellets had to go through pre-treatment before the combustion. Co-milling and co-combustion of pellets and coal has been tested and taken in use for example in UK (Colechin 2005; Rath et al. 2010). Same studies have indicated that existing power plants could substitute coal with wood pellets (Colechin 2005; Rath et al. 2010; Savolainen 2003). In general, new fuels may also have lower alkali content than the coal (Mylläri et al. 2017) which might affect corrosion risk of boiler surfaces.

Fuel characteristics, such like its chemical composition, can have high influence on the combustion and the particles formed in the combustion. This kind of effects have been observed in several studies focused on flue gas from pulverized-fuel combustion. Particles from combustion can be characterised based on their diameter, concentration and chemical composition. These characteristics may change in the flue-gas cleaning processes. Ylätalo and Hautanen (Ylätalo and Hautanen 1998) reported — for pulverized combustion of Polish coal without flue-gas cleaning — that the particle size distribution consisted of two modes, and that the mean diameter of the first particle mode was 50 nm and the mean diameter of the second mode was 300-400 nm. In addition, they observed that the mean particle size of the first mode increased slightly as an effect of electrostatic precipitator (ESP). On the other hand, Linak et al. 2002 studied the combustion of a blend of Indonesian and Australian coal and found a trimodal particle number size distribution, particle modes in 100 nm, 1000 nm and 2000 nm, when the flue gas was sampled after the electrostatic precipitator's outlet. In addition, a combustion of anthracite coal from Shanxi province produced a bimodal particle number size distribution with modes in 100 nm and 2000 nm (Yi et al. 2008). In the studies where the flue-gas cleaning has included ESP, flue-gas desulphurisation unit (FGD) and fabric filters (FF), the mean diameter of particles has been between 30 and 90 nm (Frey et al. 2014, Mylläri et al. 2016). The chemical composition of the particles from coal combustion has been reported to consist of mineral and inorganic substances originated from the coal (Frey et al. 2014; Yi et al. 2008; Linak et al. 2002; Saarnio et al. 2014). However, the flue-gas desulphurisation can increase the particulate matter originating from reagents used in the desulphurisation process (Saarnio et al. 2014).

According to the authors' knowledge, particle emissions from the co-combustion of wood pellets and coal in real-scale power plants have been studied only by Frey et al. (2014). In their study with a 4.5% share of pellets in the fuel, the mean diameter of particles was 70-90 nm after the ESP, FGD and FF, and larger when measured after the ESP. The particle number

emissions were $6.7 \cdot 10^{10}$ MJ^{-1} with electrostatic precipitator (ESP) and $7.2 \cdot 10^{10}$ MJ^{-1} with ESP, flue-gas desulphurization and fabric filters.

Atmospheric studies for coal combustion emissions (Stevens and Pierce 2013; Junkermann and Hacker 2015; Lonsdale et al. 2012; Stevens et al. 2012; Mylläri et al. 2016) have shown that the atmospheric dilution of flue gas is affected by turbulent mixing, background concentrations and source strength. In general, all the atmospheric studies have reported that the particle number concentration increases when the flue gas plume is aged, which highlights the importance of atmospheric studies when evaluating the effects of fuel changes on particle emissions.

This study focuses on characterizing the emissions from co-combustion of wood pellets and coal with a special attention on particle number size distribution and black carbon concentration. The measurements were made for a real-scale power plant combusting 10.5% of industrial quality wood pellets mixed with coal. The particle characterisation was made in two flue-gas cleaning situations. Transmission electron microscope images of the combustion particles were used to support the black carbon and particle number size distribution measurements.

Experimental

The studied power plant is a base-load station located near Helsinki city centre in Finland. The power plant consists of two boilers (each 363 MW_{th}). One of the boilers was taken in use in 1974 (boiler 1) and the other in 1977 (boiler 2). The power plant has been originally designed to combust coal but, in this study, the experiments were conducted during wood pellet-coal-mixture combustion in boiler 1; the fuel consisted of wood pellets of industrial quality (10.5% industrial pellet) and Russian coal (89.5%). Details of the industrial pellets and coal are given in Table 1. The fuel components were the same as in (Mylläri at al. 2016, Mylläri et al. 2017). The fuel mixture was pulverised in 2 grinders before combustion in six low-NO_x technology burners (Tampella/Babcock-Hitachi HTNR low-NO_x, installed in 1992-1993) and six more burners of boiler 1 were fed with the coal from 2 grinders. The grinding was affected by the pellet addition so that the mean fuel size increased from 47-62 μm (for coal) to 54-174 μm (for the industrial pellet coal mixture) (Mylläri et al. 2017). The burners situate at the front wall of the boiler. The

boiler 2 was used with Russian coal without the addition of industrial pellet. The measurements of flue gas were made simultaneously in the stack for the flue gas from the boiler 1 using wood pellet-coal mixture and in the atmosphere for the mixture of flue gases from both of the boilers.

Table 1 here

In the stack measurement, the sample was taken from the flue-gas duct in two different flue-gas cleaning situations: with and without a semi-dry flue-gas desulphurization plant (FGD, taken in use in 1991) and fabric filters (FF), later called as "FGD+FF on/off". The flue gas was cleaned with electrostatic precipitators in both of the "FGD+FF on/off" situations. The flue gas was sampled from one point close to the centre line of the flue-gas duct and diluted with a Fine Particle Sampler (FPS, Dekati Ltd., (Mikkanen and Moisio 2001)) using particle-free clean pressurized air. Total dilution ratio (DR) used in the measurements was 22 for "FGD+FF on" and 21 for "FGD+FF off". The flow inside the flue-gas duct is turbulent and it fulfills the standard EN 15259 for the measurement location. Both the dilution air and diluter were heated up to 200 ˚C to avoid nucleation in the sampling system. Particle number size distributions were measured with an Electrical Low Pressure Impactor (ELPI, Dekati Ltd., (Keskinen, J. Pietarinen, V. Lehtimäki 1992)) and a Scanning Mobility Particle Sizer (SMPS, TSI Inc., (Wang and Flagan 1990)). The SMPS consisting of a DMA3071 (TSI Inc) and a CPC3775 (TSI Inc.) was operated with 0.6/6 standard L min^{-1} flows. Particle number concentration was measured with a Condensation Particle Counter (CPC3776, TSI Inc.). A dual-spot aethalometer (AE33, Magee Scientific) with PM_1 cyclone was used to measure the aerosol light absorption at 880 nm and corresponding black carbon (BC) mass concentration in the PM_1 size fraction. Detailed information about the measurement setup for stack and atmospheric measurements are shown in Figure 1. Concentration of the gases in the diluted sample were analysed with CO_2-analyser (model VA 3100, Horiba) and NO, NO_2 and NO_x-analyser (model APNA 360, Horiba). Measurement data were also received from regulatory monitoring of the power plant emissions; raw flue-gas SO_2, NO_x, CO_2 concentrations and dust (SICK RM 230, calibrated based on SFS-EN 13284-1 standard) were measured directly inside the flue-gas duct. Measurement setup and instruments were similar than in the study of Mylläri et al 2016 (Mylläri et al. 2016). In addition to online measurements, the flue-gas particles of coal+10.5% industrial pellets combustion were

collected with a flow-through-type sampler onto holey carbon grids for microscopy studies. These particle samples were studied later with a transmission electron microscope (TEM, Jeol JEM-2010) equipped with an energy dispersive X-ray spectrometer (EDS, Noran Vantage with Si(Li) detector, Thermo Scientific). Furthermore, the amount of unburned carbon in fly ash samples collected from ESP was determined with Loss on ignition (LOI) method. Further, radiocarbon dating was used to analyse the portion of biomass-based carbon in the fly ash.

Figure 1 here

The measurements in the atmospheric flue-gas plume were made with a helicopter equipped with aerosol instruments. Measurements were conducted in 26th of March 2014 at 10:30-11:41 UTC+2 for "FGD+FF on" and 14:28-15:41 UTC+2 for "FGD+FF off" situation. During the "FGD+FF on" flight, the temperature was 6.5±0.05˚C, wind speed was 8±0.6 m/s and relative humidity 29±0.6%. Respectively during "FGD+FF off" flight, the temperature was 4.6±0.4 ˚C, wind speed was 6.25±0.4 m/s and relative humidity 38±3%. No additional dilution of the sample was needed for the measurement equipment in the helicopter because of the significant natural dilution of the flue gas in the atmosphere. The measurement instruments installed in the helicopter had high sampling frequency (1 Hz). Particle size distribution was measured with an Engine Exhaust Particle Sizer (EEPS, TSI Inc, (Mirme 1994)) and the total particle number concentration with a CPC3776 (TSI Inc.). Additionally, gaseous components CO_2/CH_4/H_2O (Cavity ring-down spectrometry Picarro model G1301-m CO_2/CH_4/H_2O flight analyser) and SO_2 (Thermo Scientific Inc. model 43i SO_2 analyser with 5 second response time) were also measured from the flue-gas plume. The position of the helicopter during the flight was recorded based on GPS-coordinates, shown in Figure SI1. Flight direction was 222˚ ± 7.2˚ during the "FGD+FF on" situation and 222˚ ± 7.3˚ during the "FGD+FF off" situation. The flue-gas plume dispersion and dilution was also measured with a Halo Photonics scanning Doppler lidar. Figure SI3 shows the cross section of the diluting plume in both of the FGD+FF cases. It should be noted that the flight measurements for "FGD+FF off" situation were interfered with a flue gas from the other boiler combusting 100% coal in "FGD+FF on" mode. The flue-gas ducts of the boilers were parallel inside the stack and, thus, the atmospheric measurements were performed for the mixed flue-gas plume.

Results

Table 2 lists the flue-gas concentrations of CO_2, SO_2, NO_x, O_2, CO, total particle number (N_{tot}) and dust measured in the stack. In addition, Table 2 shows the flow rate and the temperature of the flue gas inside the duct as well as the emission factors for particle number, dust and BC. The emission factors were calculated from total particle number, dust and BC concentrations using the measured CO_2 concentrations and multiplying that with 95.0115 g CO_2 MJ^{-1} for 10.5% industrial pellet and coal (Statistics Finland, Fuel classification 2017). All the values are presented for both studied flue-gas cleaning situations. In general, the CO_2, NO_x, O_2 concentrations and the flue-gas flow rate were relatively similar with both of the flue-gas cleaning situations. Instead, the "FGD+FF on" lowered the total particle number concentration from $(738 \pm 70)\cdot 10^3$ to 354 ± 623, thus by a factor of 2000. The dust concentration was decreased by the factor of 20 and the SO_2 concentration by the factor of four. The FGD+FF also lowered the flue-gas temperature from 129 ˚C to 77 ˚C. The CO concentrations were slightly elevated in the combustion of pellets and coal compared to coal combustion, where CO concentrations were 0 ± 0 ppm. No correlation between the two was observed in a more detailed analysis of CO and BC concentrations.

For the studied fuel, i.e., for the mixture of coal and 10.5% industrial pellet, the particle number emission factor was $3.4\cdot 10^{11}$ MJ^{-1} and the particulate mass emission factor calculated from the regulatory dust measurement results of the power plant was 50 mg MJ^{-1} in the "FGD+FF off" situation. In "FGD+FF on" situation, the particle number emission factor was around $1.7\cdot 10^8$ MJ^{-1} and particle mass emission factor around 2 mg MJ^{-1} for the mixture of coal and 10.5% industrial pellets. The emission factor for the BC was calculated from 880 nm wavelength concentration data of the aethalometer. EF_{BC} for FGD+FF off situation was $2.8\cdot 10^2$ μg/kg fuel. The usage of FGD+FF decreased the EF_{BC} to 0.33 μg/kg fuel, thus by a factor of 848. The fly ash from the combustion of industrial pellets and coal contained 10.8% of unburned carbon. The amount of biomass-originated carbon in the fly ash was 0.5%, which is thus only a small portion of the total amount of unburned carbon in fly ash. When combusting coal, the mean amount of unburned carbon was higher (12±2.8)% of the total amount of fly ash, analysed from daily samples of the whole year 2012.

Table 2 here

Mean particle number size distributions measured from the flue-gas duct are shown in Figure 2 (a). The particle number size distributions were measured in both of the studied flue-gas cleaning situations ("FGD+FF on" and "FGD+FF off") with SMPS and ELPI. However, in the "FGD+FF on" situation the raw data measured by ELPI, i.e., electric currents, were closed to noise level in submicron particle size range and thus, the particle number size distribution with the ELPI in "FGD+FF on" situation was not included into the figure. However, regardless of low particle concentration, the particle size distribution could be measured using the SMPS. Based on this measurement, in the "FGD+FF on" situation the mean electrical mobility equivalent diameter was 72 nm and the geometric standard deviation of the number size distribution was GSD 1.51, measured with SMPS. In the "FGD+FF off" situation, the mean electrical mobility equivalent diameter was 74 nm and the GSD of the size distribution was 1.46. When measured with the ELPI, the mean aerodynamic equivalent diameter of the particle number size distribution was 152 nm (GSD 1.51) for "FGD+FF off" situation. The difference in the mean diameters measured using the ELPI and the SMPS originates from the differences in the particle size classification principles of these instruments and indicates that the particles dominating the particle number size distributions have relatively high effective densities (see Ristimäki et al. 2002). Here, the effective density of particles was 2.5 g cm^{-3} when calculated based on the geometric mean diameters (GMD) of the size distributions of the particles in "FGD+FF off" situation.
The particle volume size distributions are shown in Figure 2 (b) for particles smaller than 1 μm in diameter. The particle volume size distributions show that the particles larger 100 nm in diameter significantly affect particulate volume and thus also the particulate mass concentration in the flue gas. The particle number size distributions are shown in Figure SI3 in log log scale, which shows more detailed the bimodality of the particle number size distribution.

Figure 2 here

Figure 2 also shows TEM images of the particles in both of the flue-gas cleaning situations, in "FGD+FF off" (c) and in "FGD+FF on" (d). In the "FGD+FF off" situation, three different types

of particles were observed. First, the flue gas contained large spherical particles with diameter of around 500 nm. These particles comprised mainly of inorganic species; based on the EDS analyses these particles contained Si, Al, Fe, K, Ca, Mg and Ti. The second type of particles was agglomerated particles that consisted mainly of spherical primary particles from 25 nm to 50 nm in diameter. These small primary particles in agglomerates contained Si, Al, Ca, P, Fe. In addition, Mg was found in some of these primary particles. Thirdly, there were particles that had the structure of agglomerated soot, but they also contained detectable amounts of Si, Al, P and Ca. Also these particles contained spherical primary particles (seen as dark spherical parts in particle shown in the down row on the left side in Figure 2 (c)). The particles of the second and the third type had clearly different nanostructures; in the third type particles the typical nanostructure of soot particles (see e.g. (Happonen et al. 2010)) can be seen (see Figures SI4 and SI5).

Images of particles on TEM samples collected in "FGD+FF on" situation (Figure 2 (d)) show three types of particles: relatively small particles with diameter of 100-200 nm and two types of relatively large 800-1800 nm particles. First, some of these larger particles seem to have porous surface and irregular shape (Figure (d) top row on the left side). The EDS measurements revealed that these particles consisted mainly of Ca and S, but also small amounts of Ti, Si and Mg. These porous particles had collected smaller spherical inorganic particles on their surfaces, similar to the first type of particles seen in Figure 2 (c) (top row on left side). Second, the other type of larger particles (800-1400 nm in diameter in Figure 2 (d) top row on the right side) had similar chemical composition as the spherical (large) particles in "FGD+FF off" situation (Figure 2 (c), top row on left side). These particles contained Si, Al, Mg, Ti, Fe, S and Ca. These particles had also smaller particles with agglomerated structure attached on their surfaces. It can be assumed that these particles were formed by coagulation of the large primary particles and smaller agglomerates (consisting of Si, Al, Ca, P, S, Mg, Cu, K, Ti and Fe) seen in the "FGD+FF off" situation. These primary-particle agglomerates as well as primary particles (100-200 nm) were also found on their own on the TEM grids (Figure (d), down row on right side). In general, the TEM images indicated that the flue gas contained relatively large particles in "FGD+FF on" situation, which could not be measured with the SMPS. However, the particle number size distribution and especially the particle volume size distribution measured by the SMPS indicated that there were also larger particles in the flue gas.

Figure 3 here

Like presented in the experimental section, measurements were made also in the atmosphere for the diluting flue gas. These were made with a helicopter equipped with aerosol instruments. In the data analysis, the atmospheric dilution profiles of the studied pollutants were calculated using the GPS-coordinates to determine the distance between the measurement point (helicopter position) and the stack. The atmospheric age of the flue gas was calculated using the distance and the wind speed. Each measured concentration of CO_2, SO_2 and the ΔN_{tot} (the background concentration subtracted from the measured N_{tot}) were further classified to 5-second age intervals. The resulted values are shown in Figure 3. The median values of SO_2, CO_2 and ΔN_{tot} concentrations on each 5-second time interval was plotted on the y-axis. The CO_2 and SO_2 concentrations in *ppm* and *ppb*, respectively, are shown on the left y-axis and the ΔN_{tot} (cm^{-3}) on the right y-axis. In the calculation of the ΔN_{tot} (cm^{-3}), the background particle number concentration was determined from the sampling points, which were outside the plume area marked in Figure S1. The median background concentration of particle number concentration in the atmosphere was 7330 cm^{-3} for "FGD+FF on" and 15700 cm^{-3} for "FGD+FF off".

In the "FGD+FF off" situation, the dilution profiles of gaseous CO_2 and SO_2 and the particle number concentration (ΔN_{tot}) can be clearly seen in Figure 3. All the SO_2, CO_2 and ΔN_{tot} peaked near the stack. The dilution of gaseous compounds to the background concentrations took approximately 200 seconds, which corresponds to distance less than 2 km from the stack. The dilution profile of the ΔN_{tot} was relatively similar than that of gaseous compounds; the ΔN_{tot} peaked near the flue-gas stack and diluted in 200 seconds to the background concentrations. In the "FGD+FF on" situation the dilution profiles of gaseous compounds (CO_2 and SO_2) were relatively similar like in the "FGD+FF off" situation; clear concentration peaks were measured close to the stack, and after 200 seconds the concentrations were at the background level. Instead, the profile of ΔN_{tot} differed significantly from the "FGD+FF off" situation during the first 500 seconds of dilution. First, no significant or separate peak was observed in the beginning of dilution and second, the ΔN_{tot} remained at higher concentrations for 0-500 seconds after the flue gas entered to the atmosphere. Finally, in both of the flue-gas cleaning situations, the

particle number concentration increased at the most aged part of the flue gas plume, in "FGD+FF off" after 400 seconds and in "FGD+FF on" situation after 800 seconds of atmospheric dilution.

During the data analysis, it was observed that a regional atmospheric nucleation event might affect the results in "FGD+FF off" situation. The regional nucleation event increased the particle concentrations after noon. The event was observed for example at Kumpula SMEAR III station (Junninen et al. 2009) during "FGD+FF off" measurement. Despite the nucleation event, the ΔN_{tot} was above zero concentration, thus above the background particle number concentration which included the particles from the regional nucleation event.

Figure 4 here

In the "FGD+FF off" situation, the atmospheric dilution of the flue-gas plume could be also observed from the particle number size distribution (see Figure 4 (a), plume ages up to 400 s) for particles around 40-100 nm in diameter. The measurement was made with the EEPS installed into the helicopter. Elevated concentrations of these particles with mean diameter of approximately 80 nm corresponded relatively well to the mean particle diameter measured with the SMPS for the flue gas sampled from the stack, see Figure 2. Additionally, significant number concentration of particles smaller than 30 nm in diameter were observed in the diluting flue-gas plume. For the "FGD+FF off" situation, the number concentration of particles below 30 nm in diameter was constant throughout the measurement which indicates that these particles belonged to the regional background aerosol. Instead, during the "FGD+FF on" situation no such high nanoparticle concentrations were measured in the background. Therefore, in can be assumed that the observed nanoparticles existed due to the emissions from the power plant. However, it should be keep in mind that the EEPS can suffer from an increased electrical noise in the electrometers that are used to detect particles, especially in small particle sizes and particularly in helicopter measurements were the device is exposed to vibration. Due to this reason, the any direct comparison between the N_{tot} measured by the CPC and total particle number concentration from size distributions measured with EEPS are not seen to be useful (Levin et al. 2015).

Discussion

The focus of this study was in the characterization of the emissions of a large CHP power plant fuelled with the mixture of coal and wood pellets. The special focus was in the characterization of flue-gas particles. The study has been motivated by the need to decrease the CO_2 emissions of energy production that has resulted, in general, the need to utilize biomass in existing power plant infrastructures. The study is continuation especially to the study for coal combustion emissions, presented in Mylläri et al. (2016), and the study for the effect of fuels on aerosols in boiler conditions, presented in Mylläri et al. (2017).

This study has showed that the flue gas aerosol from co-combustion of coal and wood pellets contains various types of particles. The particles have size distribution covering large particle size range. In addition to particle size, also other characteristics of particles vary significantly and, like indicated by TEM images of particles, they can be also internally mixed with each other. The flue-gas aerosol was significantly affected by the flue-gas cleaning system.

The complexity of the particle characteristics makes it difficult to evaluate all the atmospheric effects of the flue-gas aerosol and to evaluate the effects of fuel changes. If the results of this study is compared to the coal combustion study of Mylläri et al. (2016), it can be concluded that the 10.5% share of industrial pellets mixed with coal could lower power plant's particle number and particle mass emissions when the power plant uses ESPs to clean its flue gases. Based on the data presented by Mylläri et al. (2016) and by using the CO_2-release factor of 93.3 g CO_2 MJ^{-1} for coal combustion (Statistics Finland, Fuel classification 2017), for the coal combustion the particle number emission factor was $8.6 \cdot 10^{12}$ MJ^{-1} and the particle mass emission factor was 90 mg MJ^{-1} in "FGD+FF off" situation. Both are significantly higher than the emission factors measured for the combustion of the mixture industrial wood pellet and coal in this study. Thus, the co-combustion of biomass and coal can have positive effects on the emissions, at least from the air quality viewpoint. However, from particle number and mass emission point of view, the flue-gas cleaning system has even higher influence to the emissions.

Black carbon (BC) concentrations of the flue-gas aerosol can be seen important in respect of the climatic effects of flue gas. This study indicated that in the case of co-combustion of industrial pellets and coal, the flue-gas aerosol contained elevated concentrations of BC. These concentrations were, however, depended on the flue-gas cleaning so that they were approximately 0.03 μg m^{-3} in the "FGD+FF on" situation and 25.5 μg m^{-3} in the "FGD+FF off" situation. Thus, during the normal operation of the power plant, i.e., in the "FGD+FF on"

situation, the measured BC concentrations were relatively low. To compare, the BC concentrations from the exhaust of heavy duty buses have been measured to be between 1-55 μg m^{-3}, depending on the fuel and vehicle (Saarikoski et al. 2017). In Helsinki, the street level background concentration of the BC is around 1 μg m^{-3} and on road 2.9-5.5 μg m^{-3} (Pirjola et al. 2017). Thus, the BC concentrations at the street level are similar to the BC concentration level in the stack in "FGD+FF on" situation. The result highlights the important role of flue-gas cleaning in the BC emissions.

In the TEM analysis part of the study, we observed particles with a large particle size range and different characteristics. Regarding the BC emissions discussed above, we observed soot particles consisting of agglomerated spherical primary particles. The nanostructure of these primary particles was clearly similar to the nanostructure of diesel exhaust particles (see e.g. Happonen et al. 2010). In particle size distribution, these soot mode particles contributed especially in particles sizes above 100 nm. Based on the boiler aerosol study (Mylläri et al. 2017), the addition of the pellets increases particle concentrations especially in this size. Thus, in general, result indicate that agglomerated soot particles cannot be used as tracers of diesel vehicle emissions at least in environments influenced by coal and biomass combustion power plants.

In the atmospheric measurements, the flue-gas dilution time-scales for the atmospheric new particle formation were similar to those observed in Mylläri et al. (2016) for 100% coal combustion; the increase in flue-gas particle number concentration was observed after 400 seconds in the "FGD+FF off" situation and after 500 seconds in the "FGD+FF on" situation. In principle, the difference between the "FGD+FF on" and "FGD+FF off" situations in the starting of new particle formation could be explained by the higher flue-gas SO_2 concentration in the "FGD+FF off" case. This indicate, at least qualitatively, that sulphur compounds have a role the new particle formation in the atmospheric flue-gas plume, most probably by sulphuric acid formation by atmospheric oxidation of the emitted SO_2. However, our previous study (Mylläri et al. 2016) indicated that the new particle formation in the flue-gas plume could not be fully explained only by sulphuric acid nucleation.

Conclusions

In this study the focus was in the atmospheric emissions of particles and gaseous compounds from a real-scale power plant. Emissions from co-combustion of wood pellets and coal were studied with the measurements made at the power plant stack and in the atmosphere. The results from stack measurements showed that the flue-gas cleaning devices work efficiently for SO_2, particle number concentration and dust with the studied fuel mixture.

This study showed that the aerosol emitted from power plant fuelled with wood pellets and coal is relatively complicated mixture of internally and externally mixed particles. This aerosol is strongly affected by flue-gas cleaning and atmospheric processes. Importantly, the study showed elevated concentrations of black carbon (BC) in the flue gas, associated with the agglomerated soot particles found in the TEM analyses. Due to the climatic effects of BC, this observation should be taken into account when utilizing biofuels in existing power production facilities. The mean diameter of all particles in particle number size distributions was found to be between 72-75 nm in both of the flue-gas cleaning situations. The particles consisted mainly of inorganic matter, which was observed from the EDS analysis made together with the transmission electron microscopy imaging for the particles.

The co-combustion of wood pellets and coal resulted relatively similar atmospheric flue-gas plume concentrations and phenomena than previously observed for coal combustion. Especially, the observation that the total particle number concentration started to increase after 400-800 seconds after the emission should be taken into account when the emissions are evaluated in regional level.

Acknowledgements

The study was conducted in the MMEA WP 4.5.2. of Cleen Ltd., funded by Tekes (the Finnish Funding Agency for Technology and Innovation). Authors like to acknowledge Mr Aleksi Malinen for measurement help. F.M. acknowledges TUT Graduate School, KAUTE-foundation, TES-foundation for financial support. E.A., V.V. and E.O. acknowledge the support of the Academy of Finland Centre of Excellence program (project number 307331). F.M. and T.R. work has been supported by the Strategic Research Council at the Academy of Finland, project Transition to a resource efficient and climate neutral electricity system (EL-TRAN) grant number 314319.

Supporting Information includes Figures related to atmospheric conditions during measurements: lidar results and helicopter flight directions are shown from the stack measurements. In addition, CO_2, SO_2, NO_x, N_{tot} and dust concentrations in (mg Nm^{-3} or m^{-3}) reduced to 6% O_2.

References

Al-Naiema, Ibrahim, Armando D. Estillore, Imali A. Mudunkotuwa, Vicki H. Grassian, and Elizabeth A. Stone. 2015. "Impacts of Co-Firing Biomass on Emissions of Particulate Matter to the Atmosphere." *Fuel* 162 (December): 111–20. doi:10.1016/j.fuel.2015.08.054.

Colechin, Mike. 2005. "Best Practice Brochure : Co- Firing of Biomass (Main Report)," no. May.

Frey, Anna K., Karri Saarnio, Heikki Lamberg, Fanni Mylläri, Panu Karjalainen, Kimmo Teinilä, Samara Carbone, et al. 2014. "Optical and Chemical Characterization of Aerosols Emitted from Coal, Heavy and Light Fuel Oil, and Small-Scale Wood Combustion." *Environmental Science and Technology* 48 (1): 827–36. doi:10.1021/es4028698.

Hansen, P.F.B, K.H Andersen, K Wieck-Hansen, P Overgaard, I Rasmussen, F.J Frandsen, L.a Hansen, and K Dam-Johansen. 1998. "Co-Firing Straw and Coal in a 150-MWe Utility Boiler: In Situ Measurements." *Fuel Processing Technology* 54 (1–3): 207–25. doi:10.1016/S0378-3820(97)00070-2.

Happonen, Matti, Tero Lähde, Maria E. Messing, Teemu Sarjovaara, Martti Larmi, L. Reine Wallenberg, Annele Virtanen, and Jorma Keskinen. 2010. "The Comparison of Particle Oxidation and Surface Structure of Diesel Soot Particles between Fossil Fuel and Novel Renewable Diesel Fuel." *Fuel* 89 (12): 4008–13. doi:10.1016/j.fuel.2010.06.006.

Heinzel, T, V Siegle, H Spliethoff, and K R G Hein. 1998. "Investigation of Slagging in Pulverized Fuel Co-Combustion of Biomass and Coal at a Pilot-Scale Test Facility." *Fuel Processing Technology* 54: 109–25. doi:10.1016/S0378-3820(97)00063-5.

Jiménez, Santiago, and Javier Ballester. 2004. "Formation and Emission of Submicron Particles in Pulverized Olive Residue (Orujillo) Combustion." *Aerosol Science and Technology* 38 (7): 707–23. doi:10.1080/02786820490490092.

Junkermann, Wolfgang, and Jorg M. Hacker. 2015. "Ultrafine Particles over Eastern Australia:

An Airborne Survey." *Tellus, Series B: Chemical and Physical Meteorology* 67 (1): 1–18. doi:10.3402/tellusb.v67.25308.

Junninen, Heikki, Antti Lauri, Petri Keronen, Pasi Aalto, Veijo Hiltunen, Pertti Hari, and Markku Kulmala. 2009. "Smart-SMEAR: On-Line Data Exploration and Visualization Tool for SMEAR Stations." *Boreal Environment Research* 14 (4): 447–57.

Keskinen, J. Pietarinen, V. Lehtimäki, M. 1992. "Electrical Low Pressure Impactor." *Journal of Aerosol Science* 23 (4): 353–60.

Kuuluvainen, Heino, Panu Karjalainen, Cyril J E Bajamundi, Joni Maunula, Pasi Vainikka, Juha Roppo, Jorma Keskinen, and Topi Rönkkö. 2015. "Physical Properties of Aerosol Particles Measured from a Bubbling Fluidized Bed Boiler." *Fuel* 139. Elsevier Ltd: 144–53. doi:10.1016/j.fuel.2014.08.048.

Levin, M, A Gudmundsson, J H Pagels, M Fierz, K Mølhave, J Löndahl, K A Jensen, and I K Koponen. 2015. "Limitations in the Use of Unipolar Charging for Electrical Mobility Sizing Instruments: A Study of the Fast Mobility Particle Sizer." *Aerosol Science and Technology* 49 (8): 556–65. doi:10.1080/02786826.2015.1052039.

Linak, William P, C Andrew Miller, Wayne S Seames, and Jost O L Wendt. 2002. "Pulverized-Coal Combustion" 29: 441–47.

Lonsdale, C. R., R. G. Stevens, C. A. Brock, P. A. Makar, E. M. Knipping, and J. R. Pierce. 2012. "The Effect of Coal-Fired Power-Plant SO2 and NOx Control Technologies on Aerosol Nucleation in the Source Plumes." *Atmospheric Chemistry and Physics* 12 (23): 11519–31. doi:10.5194/acp-12-11519-2012.

Madanayake, Buddhike Neminda, Suyin Gan, Carol Eastwick, and Hoon Kiat Ng. 2017. "Biomass as an Energy Source in Coal Co-Firing and Its Feasibility Enhancement via Pre-Treatment Techniques." *Fuel Processing Technology* 159: 287–305. doi:10.1016/j.fuproc.2017.01.029.

Mikkanen, Pirita, and Mikko Moisio. 2001. "Sampling Method for Particle Measurements of Vehicle Exhaust," no. 724: 1–6.

Mirme, A. 1994. "Electric Aerosol Spectrometry." Tartu University.

Mylläri, F., E. Asmi, T. Anttila, E. Saukko, V. Vakkari, L. Pirjola, R. Hillamo, et al. 2016. "New Particle Formation in the Fresh Flue-Gas Plume from a Coal-Fired Power Plant: Effect of Flue-Gas Cleaning." *Atmospheric Chemistry and Physics* 16 (11). doi:10.5194/acp-16-

7485-2016.

Mylläri, F., P. Karjalainen, R. Taipale, P. Aalto, A. Häyrinen, J. Rautiainen, L. Pirjola, R. Hillamo, J. Keskinen, and T. Rönkkö. 2017. “Physical and Chemical Characteristics of Flue-Gas Particles in a Large Pulverized Fuel-Fired Power Plant Boiler during Co-Combustion of Coal and Wood Pellets.” *Combustion and Flame* 176. doi:10.1016/j.combustflame.2016.10.027.

Mylläri, Fanni, Eija Asmi, Tatu Anttila, Erkka Saukko, Ville Vakkari, Liisa Pirjola, Risto Hillamo, et al. 2016. “New Particle Formation in the Fresh Flue-Gas Plume from a Coal-Fired Power Plant: Effect of Flue-Gas Cleaning.” *Atmospheric Chemistry and Physics* 16 (11): 7485–96. doi:10.5194/acp-16-7485-2016.

Nutalapati, D., R. Gupta, B. Moghtaderi, and T. F. Wall. 2007. “Assessing Slagging and Fouling during Biomass Combustion: A Thermodynamic Approach Allowing for Alkali/ash Reactions.” *Fuel Processing Technology* 88 (11–12): 1044–52. doi:10.1016/j.fuproc.2007.06.022.

Piotrowska, Patrycja, Alejandro Grimm, Nils Skoglund, Christoffer Boman, Marcus Öhman, Maria Zevenhoven, Dan Boström, and Mikko Hupa. 2012. “Fluidized-Bed Combustion of Mixtures of Rapeseed Cake and Bark: The Resulting Bed Agglomeration Characteristics.” *Energy and Fuels* 26 (4): 2028–37. doi:10.1021/ef300130e.

Pirjola, Liisa, Jarkko V. Niemi, Sanna Saarikoski, Minna Aurela, Joonas Enroth, Samara Carbone, Karri Saarnio, et al. 2017. “Physical and Chemical Characterization of Urban Winter-Time Aerosols by Mobile Measurements in Helsinki, Finland.” *Atmospheric Environment* 158: 60–75. doi:10.1016/j.atmosenv.2017.03.028.

Pisa, Ionel, and Gheorghe Lazaroiu. 2012. “Influence of Co-Combustion of Coal/biomass on the Corrosion.” *Fuel Processing Technology* 104: 356–64. doi:10.1016/j.fuproc.2012.06.009.

Rath, John, Samson Kay, David Bielunis, Rick Pellage, and John Rath. 2010. “Technical Publication: Co-Milling and Suspension Co-Firing of Wood Pellets with Bituminous Coal.”

Ristimäki, Jyrki, Annele Virtanen, Marko Marjamäki, Antti Rostedt, and Jorma Keskinen. 2002. “On-Line Measurement of Size Distribution and Effective Density of Submicron Aerosol Particles.” *Journal of Aerosol Science* 33 (11): 1541–57. doi:10.1016/S0021-8502(02)00106-4.

Saarikoski, S, H Timonen, S Carbone, H Kuuluvainen, J V Niemi, A Kousa, T Rönkkö, D

Worsnop, R Hillamo, and L Pirjola. 2017. “Investigating the Chemical Species in Submicron Particles Emitted by City Buses.” *Aerosol Science and Technology* 51 (3). Taylor & Francis: 317–29. doi:10.1080/02786826.2016.1261992.

Saarnio, Karri, Anna Frey, Jarkko V. Niemi, Hilkka Timonen, Topi Rönkkö, Panu Karjalainen, Mika Vestenius, et al. 2014. “Chemical Composition and Size of Particles in Emissions of a Coal-Fired Power Plant with Flue Gas Desulfurization.” *Journal of Aerosol Science* 73: 14–26. doi:10.1016/j.jaerosci.2014.03.004.

Savolainen, Kati. 2003. “Co-Firing of Biomass in Coal-Fired Utility Boilers” 74: 369–81. doi:10.1016/S0306-2619(02)00193-9.

Sevonius, Christoffer, Patrik Yrjas, and Mikko Hupa. 2014. “Defluidization of a Quartz Bed – Laboratory Experiments with Potassium Salts.” *Fuel* 127 (July): 161–68. doi:10.1016/j.fuel.2013.10.047.

Statistics Finland, Fuel Classification 2017, http://www.stat.fi/polttoaineluokitus. Accessed 29.11.2017

Stevens, R. G., and J. R. Pierce. 2013. “A Parameterization of Sub-Grid Particle Formation in Sulfur-Rich Plumes for Global- and Regional-Scale Models.” *Atmospheric Chemistry and Physics* 13 (23): 12117–33. doi:10.5194/acp-13-12117-2013.

Stevens, R. G., J. R. Pierce, C. A. Brock, M. K. Reed, J. H. Crawford, J. S. Holloway, T. B. Ryerson, L. G. Huey, and J. B. Nowak. 2012. “Nucleation and Growth of Sulfate Aerosol in Coal-Fired Power Plant Plumes: Sensitivity to Background Aerosol and Meteorology.” *Atmospheric Chemistry and Physics* 12 (1): 189–206. doi:10.5194/acp-12-189-2012.

Strzalka, Rafal, Dietrich Schneider, and Ursula Eicker. 2017. “Current Status of Bioenergy Technologies in Germany.” *Renewable and Sustainable Energy Reviews* 72: 801–20. doi:10.1016/j.rser.2017.01.091.

Tolvanen, Henrik, Tiina Keipi, and Risto Raiko. 2016. “A Study on Raw, Torrefied, and Steam-Exploded Wood: Fine Grinding, Drop-Tube Reactor Combustion Tests in N2/O2 and CO2/O2 Atmospheres, Particle Geometry Analysis, and Numerical Kinetics Modeling.” *Fuel* 176: 153–64. doi:10.1016/j.fuel.2016.02.071.

Vainio, Emil, Patrik Yrjas, Maria Zevenhoven, Anders Brink, Tor Laur??n, Mikko Hupa, Tuula Kajolinna, and Hannu Vesala. 2013. “The Fate of Chlorine, Sulfur, and Potassium during Co-Combustion of Bark, Sludge, and Solid Recovered Fuel in an Industrial Scale BFB Boiler.” *Fuel Processing Technology* 105. Elsevier B.V.: 59–68.

doi:10.1016/j.fuproc.2011.08.021.

Verma, Munna, Chanchal Loha, Amar Nath Sinha, and Pradip Kumar Chatterjee. 2017. “Drying of Biomass for Utilising in Co-Firing with Coal and Its Impact on Environment – A Review.” *Renewable and Sustainable Energy Reviews* 71 (May): 732–41. doi:10.1016/j.rser.2016.12.101.

Wang, Shih Chen, and Richard C. Flagan. 1990. “Scanning Electrical Mobility Spectrometer.” *Aerosol Science and Technology* 13 (2): 230–40. doi:10.1080/02786829008959441.

Yi, Honghong, Jiming Hao, Lei Duan, Xiaolong Tang, Ping Ning, and Xinghua Li. 2008. “Fine Particle and Trace Element Emissions from an Anthracite Coal-Fired Power Plant Equipped with a Bag-House in China.” *Fuel* 87 (10–11): 2050–57. doi:10.1016/j.fuel.2007.10.009.

Ylätalo, Sampo I., and Jukka Hautanen. 1998. “Electrostatic Precipitator Penetration Function for Pulverized Coal Combustion.” *Aerosol Science and Technology* 29 (1): 17–30. doi:10.1080/02786829808965547.

About the Authors

Fanni Mylläri is a doctoral student, **Jorma Keskinen** is a professor and **Topi Rönkkö** is a research manager at Tampere University of Technology. **Erkka Saukko** was a doctoral student at TUT but now works as a senior R&D engineer at Pegasor.

Liisa Pirjola works as a project leader in Metropolia University of Applied Sciences.

Heikki Lihavainen is a former head of a unit at Finnish Meteorological Institute and is now working as a director at SIOS-Svalbard Integrated Arctic Earth Observing System. **Eija Asmi** was a group leader at FMI and is also working at Servicio Meteorológico Nacional in Buenos Aires, Argentina. **Tuomas Laurila** is a research scientist at FMI. **Ville Vakkari** is a researcher at FMI. **Ewan O’Connor** is a tenure track professor at FMI.

Jani Rautiainen works as a process engineer at Helen Oy. **Anna Häyrinen** is an air quality engineer at Helen Oy.

Ville Niemelä works as a Director, Research and Development, and Manufacturing in Dekati Ltd.

Joni Maunula works as a product engineer in Valmet Technologies.

Corresponding Author

*fanni.myllari@tut.fi, +358 40 198 1181, Korkeakoulunkatu 3, FI-33720 TAMPERE, Finland

Author Contributions

The manuscript was written through contributions of all authors. All authors have given approval to the final version of the manuscript.

Notes

The authors declare no competing financial interest.

Tables

Table 1 Properties of coal and industrial pellets (Mylläri et al. 2017)

Properties	Unit	Industrial pellet	Coal
Moisture	%	6.7	11.0-11.3
Ash	%	0.8	10.5-11.4
Volatiles	%	78.1	32.8-33.1
Heating value	GJ/t	17.7	24.6-24.9
C	%	47.4	62.3-63.1
H	%	5.6	4.1-4.2
N	%	0.1	1.8-2
O	%	39.4	0
S	mg/kg dry	180	3100-4600
Cl	mg/kg dry	39	236
Ca	mg/kg dry	2300	4300-4800
Mg	mg/kg dry	280	1700-1900
Na	mg/kg dry	69	1400-1600
K	mg/kg dry	760	2500-2900
Fe	mg/kg dry	140	4800-5700
Al	mg/kg dry	130	14200-15000
Ti	mg/kg dry	8.8	600-640
Ba	mg/kg dry	26	270-280
B	mg/kg dry	<40	210-230
Ag	mg/kg dry	<0.5	<0.5
As	mg/kg dry	<0.5	4.9-14
Be	mg/kg dry	<0.5	<0.5
Bi	mg/kg dry	<0.7	<0.7
Cd	mg/kg dry	0.2	0.1
Co	mg/kg dry	<0.5	1.4-2.1
Cr	mg/kg dry	1.2	9.7-11
Cu	mg/kg dry	1.6	7.8-8.5
Li	mg/kg dry	<0.5	9.3-10
Mn	mg/kg dry	140	38-66
Mo	mg/kg dry	<0.5	1.1-1.3

Ni	mg/kg dry	<0.5	4.1-6.6
Pb	mg/kg dry	<0.5	3.4-4.1
Rb	mg/kg dry	2.5	5.2-9.0
Sb	mg/kg dry	<0.5	<0.5
Se	mg/kg dry	<0.7	<0.7-1.1
Sr	mg/kg dry	5.5	150-170
Th	mg/kg dry	<0.5	1.2-1.3
Tl	mg/kg dry	<0.5	<0.5
U	mg/kg dry	<0.5	<0.5-0.6
V	mg/kg dry	<0.5	13-15
Zn	mg/kg dry	30	11-18

Table 2 Flue-gas concentrations of CO_2, SO_2, NO_x, O_2, CO, total particle number ($N_{tot,\ >2.5nm}$), dust, flue-gas flow rate and temperature in the stack during the measurements. Mean values (±standard deviation) are presented for both flue-gas cleaning situations ("FGD+FF off" and "FGD+FF on") for coal + 10.5% industrial pellet. Emission factors for BC_{PM1} (EF_{BC}, ng MJ^{-1}) as well as emission factors for particle number and mass (MJ^{-1} and μg MJ^{-1}) are shown for co-combustion situation and coal combustion situation. See supplementary table SI1 for CO_2, SO_2, NO_x, $N_{>2.5nm}$ and dust concentrations in (mg Nm^{-3} or m^{-3}) when reduced to 6% O_2.

	coal + 10.5 % pellet FGD+FF off	coal + 10.5 % pellet FGD+FF on
CO_2 (%)	10.6 ± 0.13	10.3 ± 0.16
SO_2 (ppb)	256 000 ± 61 400	59 900 ± 7 200
NO_x (ppm)	260 ± 8.1	260 ± 8.1
O_2 (%)	5.9 ± 0.2	5.9 ±0.12
CO (ppm)	33 ± 31	2.4 ± 8
$N_{>2.5nm}$ (cm^{-3})	$(738 \pm 70)\cdot 10^3$	354 ± 623
$EF_{N>2.5nm}$ (1 MJ^{-1})	$4.4\cdot 10^{11}$	$1.7\cdot 10^{8}$
Dust (mg Nm^{-3})	110 ± 13	5 ± 2
EF_{PM} (mg MJ^{-1})	50	2
Temperature (˚C)	129 ± 5	77 ± 7
Flow ($Nm^3\ h^{-1}$)	$(461 \pm 4.2)\cdot 10^3$	$(457 \pm 9.6)\cdot 10^3$

EF_{BC} (880nm) ng MJ^{-1}	11 470	14

Figure captions

Figure 1. (a) Measurement setup used in stack measurements. (b) Measurement setup installed in the helicopter.

Figure 2. (a) Particle number size distribution of solid particles measured at the stack in "FGD+FF on/off" situations with ELPI and SMPS (b) particle volume size distribution calculated from SMPS and ELPI results (c) TEM images of particles collected on TEM grids in "FGD+FF off" and (d) "FGD+FF on" situations. The mixture of industrial pellet and coal was used as a fuel in the experiment.

Figure 3. Concentration of CO_2 (black line, ppm, y-axis on the left), SO_2 (blue line, ppb, y-axis on the left) and ΔN_{tot} (red line, 1 cm^{-3}, y-axis on the right) in flue gas plume diluting in the atmosphere as a function of flue-gas plume age after the emission from stack. ΔN_{tot} is the particle number concentration in the flue-gas plume after subtracting the background particle number concentration from measured values. The grey vertical lines present the 2 km distance from the stack. The mixture of 10.5% industrial pellet and coal was used as a fuel in the experiment.

Figure 4. Median particle number size distribution measured from the atmosphere with helicopter in "FGD+FF off/on" (upper/lower) situations. The measurement data was classified to 5 second time intervals based on the plume age. Measurements were made with EEPS. The mixture of industrial pellets and coal was used as a fuel during the experiment.

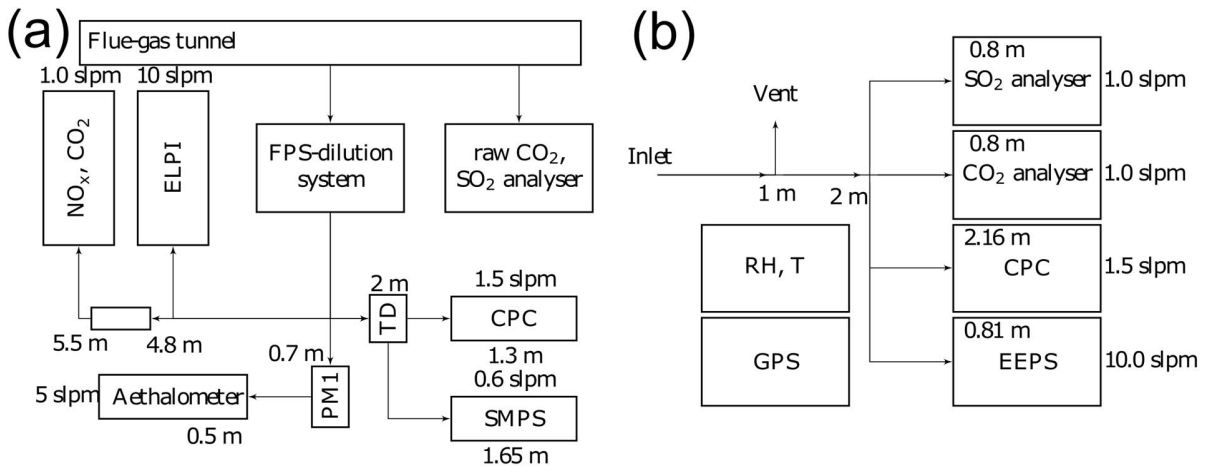
(a)
Flue-gas tunnel
1.0 slpm
10 slpm
NOx, CO2
ELPI
FPS-dilution system
raw CO2, SO2 analyser
2 m
1.5 slpm
TD
CPC
1.3 m
5.5 m
4.8 m
0.7 m
0.6 slpm
5 slpm
Aethalometer
PM1
SMPS
0.5 m
1.65 m
(b)
Vent
Inlet
1 m
2 m
0.8 m
SO2 analyser
1.0 slpm
0.8 m
CO2 analyser
1.0 slpm
2.16 m
CPC
1.5 slpm
RH, T
GPS
0.81 m
EEPS
10.0 slpm

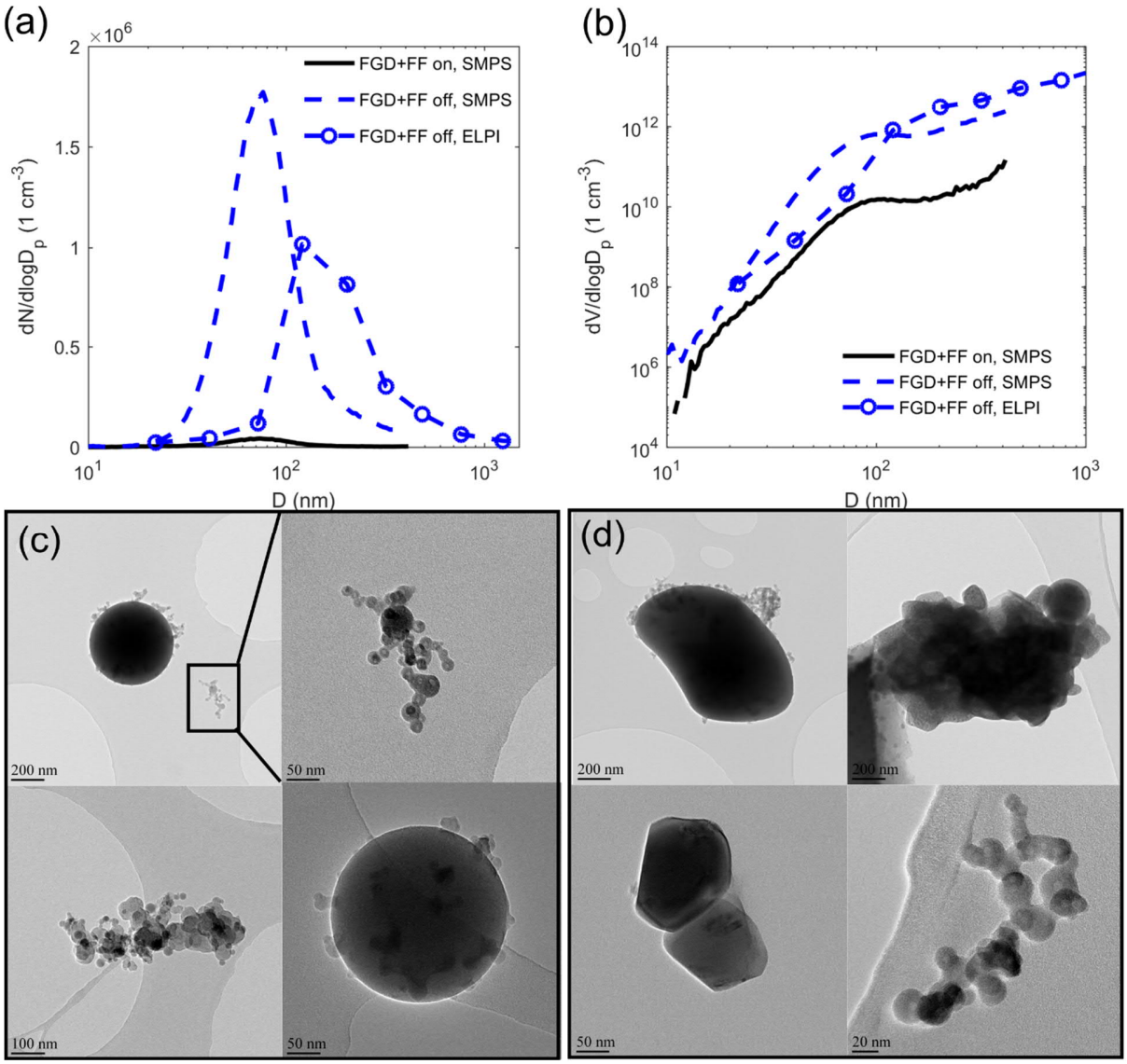
(a)
×10^6
2
1.5
1
0.5
0
dN/dlogD_p (1 cm^-3)
FGD+FF on, SMPS
FGD+FF off, SMPS
FGD+FF off, ELPI
10^1
10^2
10^3
D (nm)
(b)
10^14
10^12
10^10
10^8
10^6
10^4
dV/dlogD_p (1 cm^-3)
FGD+FF on, SMPS
FGD+FF off, SMPS
FGD+FF off, ELPI
10^1
10^2
10^3
D (nm)
(c)
200 nm
50 nm
100 nm
50 nm
(d)
200 nm
200 nm
50 nm
20 nm

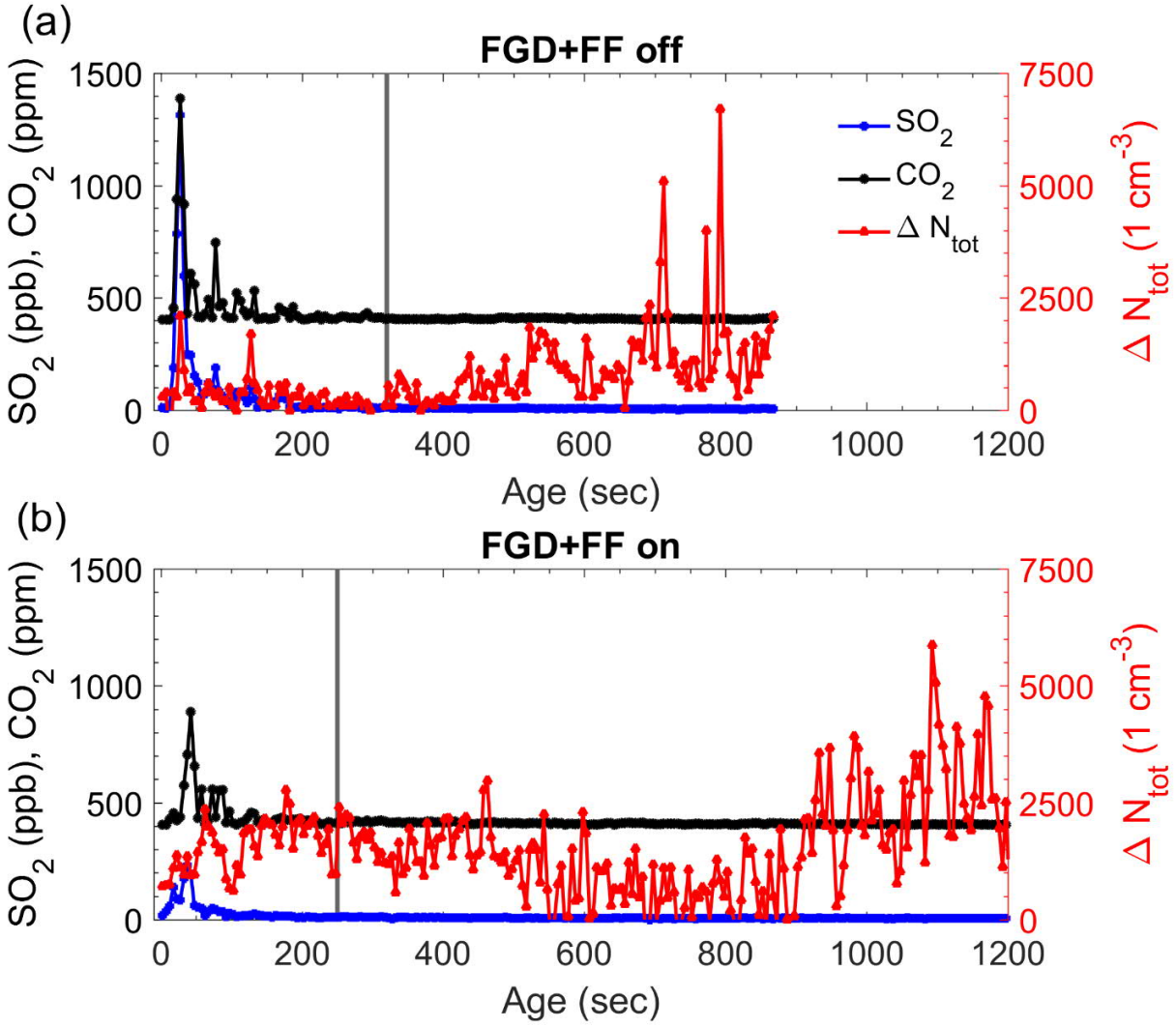
(a)
FGD+FF off
SO2 (ppb), CO2 (ppm)
ΔNtot (1 cm-3)
SO2
CO2
Δ Ntot
Age (sec)
(b)
FGD+FF on
SO2 (ppb), CO2 (ppm)
ΔNtot (1 cm-3)
Age (sec)

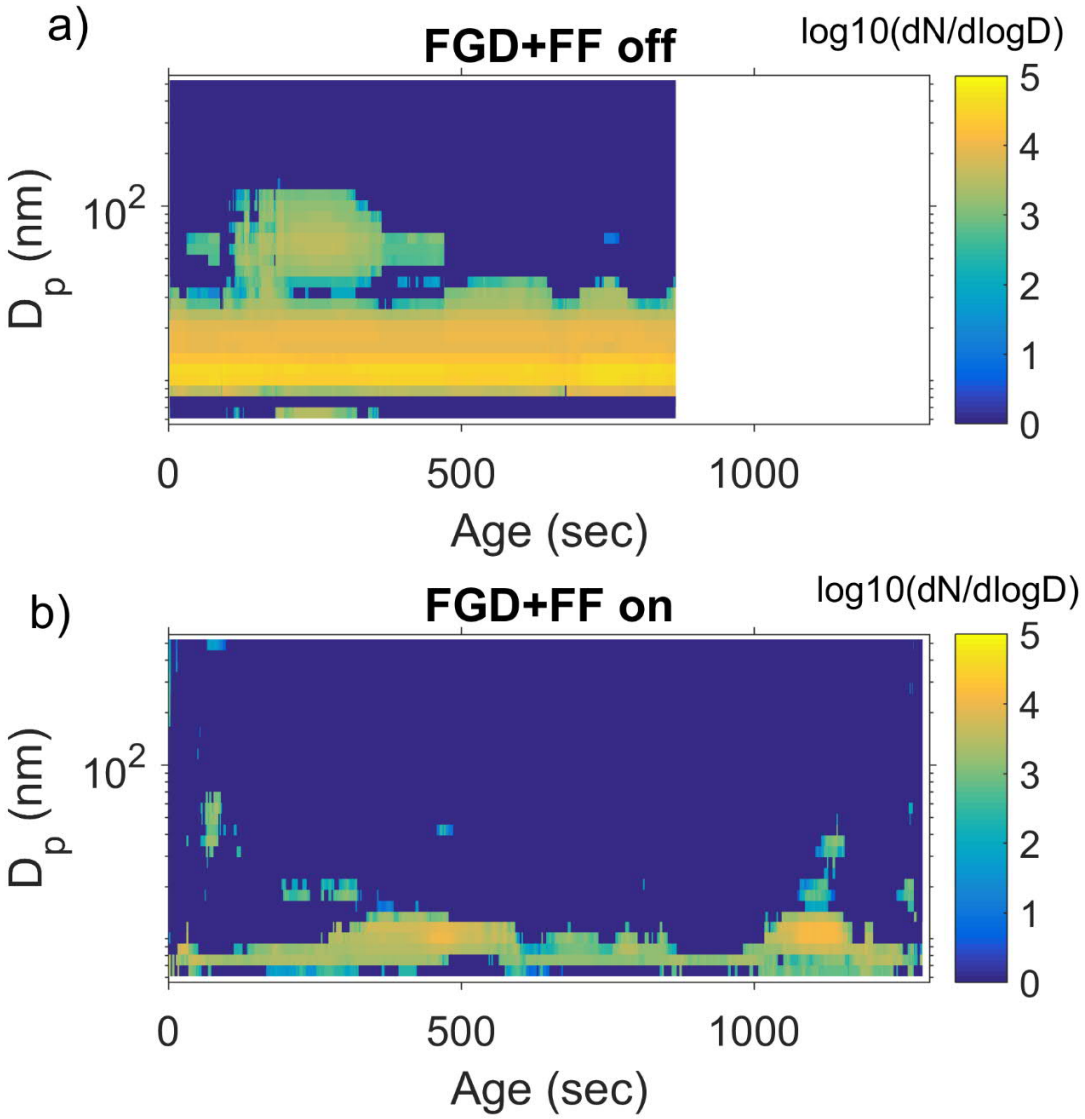
a)
FGD+FF off
log10(dN/dlogD)
5
4
3
2
1
0
D_p (nm)
10^2
0
500
1000
Age (sec)
b)
FGD+FF on
log10(dN/dlogD)
5
4
3
2
1
0
D_p (nm)
10^2
0
500
1000
Age (sec)